Proceedings World Geothermal Congress 2000
Kyushu - Tohoku, Japan, May 28 - June 10, 2000

TRACER RESPONSES IN GAS-LIQUID, TWO-PHASE FLOW THROUGH POROUS MEDIA

D. Haga[1], Y. Niibori[2], and T. Chida[1]

[1]Department of Geoscience and Technology, Graduate School of Engineering, Tohoku University, Sendai, Japan

[2]Department of Quantum Science and Energy Engineering, Graduate School of Engineering, Tohoku University, Sendai, Japan

Key Words: Two-phase flow, Bubble flow, Tracer responses, Dispersion, Porous media, Reservoir evaluation

ABSTRACT

Tracer responses in gas-liquid, two-phase flow through a fractured layer are discussed. Experiments were carried out using a glass bead bed in a cylinder. In the results, over a wide range of flow conditions of particle size, fluids-flow velocity, and water saturation (S_w), one of three types of liquid- and gas-flow pattern was obtained: a single-phase (water) flow with entrapped gases, a bubble flow, and a channel flow. Tracer tests were performed for each flow type in the bed to obtain breakthrough curves for the water phase, which determined the *hydrodynamic dispersion* coefficient (D_h) being compared with the numerical model described by a one-dimensional *advection*-dispersion equation. In a relationship between the dispersion coefficient and water saturation, critical water saturation was observed, which depended on whether or not the gas phase in the bed is mobile. Above the critical saturation, there was a single-phase (water) flow with entrapped gases, and the dispersion coefficient linearly increased as S_w decreased. Below the critical saturation, water- and gas-phase flow (channel flow) appeared. The relationship was characterized by a steep increase in D_h as S_w decreases. In the bubble flow, gases flow unsteadily in porous media as bubbles, so flow paths of water become more complex. However, the dispersion coefficients obtained by tracer experiments show that the bubble flow and unsteady fluids paths do not have serious effects on *hydrodynamic dispersion*.

1.INTRODUCTION

Tracer testing is an important technique for estimating interaction between two or more wells in a geothermal reservoir. By analyzing the tracer responses, we can obtain the permeability of fast flow-paths in a reservoir and the mean fluid residence time. Recently, studies under the condition of two-phase flow have been discussed (e.g., Gelhar et al., 1992; Niibori et al., 1996; Chen et al., 1996; Tokunaga and Wan, 1997). However, the fluid-flow is very complex in a reservoir and it is difficult to interpret tracer test results.

A tracer, which is a chemical compound, generally moves through some processes. Among them, *advection* and *hydrodynamic dispersion* are primary physical processes. These processes through porous or fractured layer are focused in many diverse fields of science and engineering. In general, *advection* describes mass transport due to the bulk movement of fluids. *Hydrodynamic dispersion* also plays an important role in a reservoir because, *hydrodynamic dispersion* determines the shape of the breakthrough curve (peak height or spread). This in turn provides some insights to the behavior of fluid flow in the reservoir, i.e., the degree of mechanical mixing through the connected flow-paths multiply with each other.

In two-phase flow condition, breakthrough curves have an eary peak and long tailing (Bond and Philips, 1990; Bond and Wierenga, 1990; Smedt and Wierenga, 1978, 1979a, 1979b, and 1984). The breakthrough curves are different from that observed under a condition of single-phase flow, however, effects of *hydrodynamic dispersion* on a breakthrough curve under a condition of two-phase flow have not been sufficiently investigated. It remains difficult to understand differences of values of *hydrodynamic dispersion* coefficient between single-phase flow and two-phase flow.

In single-phase flow, Levenspiel (1972) showed that the dispersion intensity was nearly proportional to the mean axial velocity and the particle size, by introducing an intensity of dispersion in saturated packed beds based on various experiments. Two-phase flow through porous media or fractured layer has several types of fluids-flow pattern. Haga et al. (1999) showed the effect of gas flow pattern on *hydrodynamic dispersion*. However, *hydrodynamic dispersion* coefficients for the two-phase flow has not been sufficiently investigated, e.g., effect of particle size was not discussed in Haga et al. (1999). In addition, little is known about *hydrodynamic dispersion* under a condition of bubble flow that appeared in the bed when using a relatively large scale of particle diameter.

The purpose of this study was to understand key features of *hydrodynamic dispersion* in unsaturated porous media. To determine the *hydrodynamic dispersion* coefficients, the experimental responses were compared with the numerical results of a one-dimensional *advection*-dispersion equation.

2. EXPERIMENTS

2.1 Experimental Apparatus

Figure 1 shows schematic diagram of experimental apparatus. All

experiments were carried out using methods closely similar to those described by Haga et al. (1999). A few parts of the apparatus were modified in this study. Over flow of gas was removed. Gas flow rates were adjusted using a needle bulb. Real-time processes using a personal computer measured tracer concentration.

An ideal medium, i.e., a cylinder filled with glass beads was used in the experiments. Pure water was injected continuously into the bed from the bottom at a constant flow rate using a roller pump. The packed bed was made from an acrylic cylinder 52.0 cm long and with an inside diameter of 4.1 cm. Glass beads were packed into the column. The average diameter of glass beads used in this study was 0.2 cm, 0.1 cm, or 0.06 cm.

2.2 Experimental Procedure

The tracer used in experiments was 5.0 ml of KCl solution (0.05 mol/l). The tracer was injected with a syringe within 5% of a space-time of a packed bed. The space-time was estimated by water-filled pore volume and water flow rate. The injection point was at the silicon tube that was connected to the bed at the inlet. The actual concentration of the tracer at the inlet was calculated, based on the water flow rate, the concentration of the tracer in the syringe and the injection time. At the outlet, an electrical conductivity meter (TOA Electronics, CM40V) measured the electrical conductivity of water and a personal computer calculated the concentration of KCl solution by real-time processes. After the tracer test, water saturation was determined by weighing.

2.3 Fluids Flow Conditions

In this study, tracer experiments were performed in order to examine the effects of the non-wetting fluids flow pattern on the solute transport in the wetting fluid. The tracer experiments were carried out under the following four flow conditions: single-phase flow, single-phase flow with entrapped gas, bubble flow, and channel flow. Figure 2 shows a schematic illustration of these fluid flow patterns of water and gas, as wetting and non-wetting fluids, respectively.

Figure 2(a) shows schematic illustrations of the single-phase flow condition. In this condition, only water flows continuously through the bed that is completely saturated with water. Figure 2(b) shows the condition of the single-phase flow with entrapped gases. When a liquid wets a porous medium, without previously evacuating the pore space, gases are entrapped in the porous medium as shown in figure 2(b). The gases are called the entrapped gases. The maximum wetted-phase saturation, i.e. residual water saturation, is always less than 1.0, mostly near 0.8. In this condition, water flows continuously through the bed with partially entrapped gases. Figure 2(c) shows bubble flow condition, where almost all gases exist as mobile gases. The gases flow through the bed as bubbles, while water flows continuously in the bed. Figure 2(d) shows channel flow condition, where water and gas flow continuously through the bed.

3. MATHEMATICAL MODEL

3.1 Governing Equations

The governing equation modeling the flow of a non-reactive tracer through a uniform porous medium for steady-state flow is the well-known advection-dispersion equation, which can be written in one-dimensional form as follows:

$$\varepsilon S_w \frac{\partial c_w}{\partial t} = D_{hw} \frac{\partial^2 c_w}{\partial z^2} - u_w \frac{\partial c_w}{\partial z} \tag{1}$$

where c_w is the solute concentration in the water(mol/m^3), S_w is the water saturation(m^3/m^3), ε is the porosity of the porous medium(m^3/m^3), u_w is the Darcy flux(m/s) of the water, D_{hw} is the *hydrodynamic dispersion* coefficient (m^2/s) of the solute in the water phase, t is time(s), and z is the space coordinate(m). The dimensionless form of equation (1) is

$$\frac{\partial C_w}{\partial T} = \frac{\zeta}{P_e} \frac{\partial^2 C_w}{\partial Z^2} - \frac{\partial C_w}{\partial Z} \tag{2}$$

where $Z=z/L$, $C_w=(c_w-c_b)/(c_{w0}-c_b)$, $T=t/t^*$ and $\zeta=d_p/L$. c_b is the background concentration, t^* is the space time($=L\varepsilon S_w/u_w$), ζ is the ratio of d_p to L, d_p is the particle diameter (m), and L is the length of the column(m). P_e is the Peclet number defined by

$$P_e = \frac{d_p (u_w/\theta_w)}{(D_{hw}/\theta_w)} = \frac{d_p u_w}{D_{hw}}, \quad \theta_w = \varepsilon S_w \tag{3}$$

where θ_w is the volumetric fraction of the water phase. In this study, equation (2) is used to describe the advection and dispersion of KCl solution through an unsaturated porous medium.

3.2 Initial and Boundary Conditions

The initial conditions and tracer injection are described by

$$T=0,\ C_w=0,\ in\ 0<Z<1 \tag{4}$$

$$0<T<T_{in},\ C_w=1,\ at\ Z=0 \tag{5}$$

$$T<0,\ T_{in}<T,\ C_w=0,\ at\ Z=0 \tag{6}$$

where T_{in} is the injection time of the tracer.

The boundary conditions are

$$C_{w-} = C_{w+} - \frac{\zeta}{P_e} \frac{\partial C_w}{\partial Z}\bigg|_{Z=0+}, \qquad at \qquad Z=0 \tag{7}$$

$$\frac{\partial C_w}{\partial Z} = 0, \quad at \quad Z = 1 \qquad (8)$$

where C_{w-} and C_{w+} are the tracer concentration at $Z=0^-$ and $Z=0^+$, respectively. Equation (7) is the so-called "closed-vessel boundary condition", which is applicable to a system which has a larger back-mixing magnitude than the surroundings, e.g. at the inlet of the column (Wehner and Wilhelm, 1956; Levenspiel, 1972).

3.3 Numerical Method and Parameter Estimation

The equations of (2), and (4)-(8) were solved using a forward-time central-space finite difference method. It is well known that the use of standard numerical techniques can lead to numerical oscillations in the advective-dominant system. The experimental condition in this study is a relatively advective-dominant case of the solute transport. To prevent the numerical oscillations, the third-order upwind difference method was applied in numerical calculation (Haga et al., 1999).

The unknown parameter in the governing equations is only Peclet number, P_e, in the equation (2). This study selected the value of P_e on the basis of several trials to fit data, using the SIMPLEX method (Haga et al., 1998). Sum of the residual mean square of concentration at each time was used as an objective function. The parameter was fitted so as to decrease the value of the function by the SIMPLEX method.

4. RESULTS AND DISCUSSION

4.1 Fluid Flow Patterns in Porous Media

Effects of the non-wetting fluids flow pattern on the solute transport in the wetting fluid were determined in this study. One of four types of fluids flow patterns appeared in the packed bed over a wide range of conditions of particle diameter and water saturation (S_w). Table 1 shows the observed flow patterns of fluids and experimental conditions.

In the experiments, three sizes of the particle diameter are applied. For particle diameters of 0.10 cm and 0.06 cm, single-phase flow was observed at S_w=1. Also, single-phase flow with entrapped gases was observed when water was injected into a porous medium without previously evacuating gases in the pore space. The gases were entrapped in the porous medium. The water saturation was more than 0.73 in this study. Channel flow appeared when water and gas were injected continuously from the bottom of the packed bed. For particle diameter of 0.20 cm, another flow pattern, i.e. bubble flow, appeared in addition to the three flow patterns. Two fluid flow patterns, i.e., the bubble flow (at relatively high water saturation, Sw=0.8 and 0.76) and channel flow (at low water saturation, Sw<0.7), were obtained when water and gas were injected in case of 0.20 cm particle diameter.

A critical factor affecting the flow pattern at a given location, whether the bubble flow is appeared or not, is the grain size of the porous medium (Brooks et al, 1997). A change in the flow pattern occurs around 0.1 to 0.2 cm grain diameters, with air channels occurring below the transition size and bubbles above. Brooks et al. (1997) suggested that for a given gas-liquid-solid system, there is a critical scale which dictates the dominant force, and the dominant force will in turn dictate the flow pattern. In this study, both the bubble flow and the channel flow appeared at d_p=0.2. This matches the results of Brooks et al. (1997). Our results show that the water saturation is also the critical factor that divides the two flow patterns (Fig.4). However, it is beyond of the scope of this paper to further evaluate these factors.

4.2 Experimental and Numerical Breakthrough Curves

Figure 3 compares the experimental and numerical results in case of d_p=0.2. The longitudinal axis and the horizontal axis show the normalized concentration of the KCl solution and normalized time, respectively. Each area of the normalized responses is 1. The value of Darcy flux, u_w, is 3.79×10^{-4} m/s. In this figure, the values of S_w are 1.0, 0.94, 0.82, and 0.73 for the conditions of the single-phase flow, single-phase flow with entrapped gases, bubble flow, and channel flow, respectively. When the flow condition is an advective-dominant stage, a breakthrough curve becomes sharp and has a high peak. On the other hand, a breakthrough curve becomes broad and has a low peak in case of the dispersion-dominant stage. Thus, in the single-phase flow, as shown in Fig.3, the intensity of dispersion is lowest of the four types of flow patterns. Further, intensity of dispersion is highest in the channel flow.

In order to estimate the intensity of the *hydrodynamic dispersion* for each flow pattern, the experimental responses are fitted with the numerical responses by the mathematical model. The parameters in the equations are P_e, ζ, and T_{in}. Based on the experimental conditions, the values of ζ and T_{in} are calculated. P_e is the unknown parameter in the mathematical model. The Peclet number defines the ratio of the two intensities, i.e. *advection* and *hydrodynamic dispersion*, of driven force when a solute moves through the bed. Figure 3 shows good agreement when the P_e is 0.81, 0.74, 0.62 and 0.30 for the flow conditions single-phase flow, single-phase flow with entrapped gases, bubble flow, and channel flow, respectively. These results show that P_e decreases as S_w decreases. To determine the effect of S_w on P_e, additional tracer experiments were conducted for different values of S_w.

4.3 *Hydrodynamic dispersion* in porous media

In this study tracer experiments were conducted for bubble flow in addition to the three flow conditions applied in Haga et al. (1999) for the four flow conditions. The results of Haga et al. (1999) for d_p=0.1 are also shown in this figure. Haga et al. (1999) showed that the value of P_e takes a constant value in the range of 0.75 to 0.87 for single-phase flow condition. For the condition of single-phase flow with entrapped gases, P_e decreases linearly as S_w

decreases. For channel-flow condition, the rate of the decrease in P_e is different from that in the single-phase flow with entrapped gases. P_e declines sharply at S_w values of 0.83 to 0.75, but declines gradually as S_w decreases at S_w values of 0.75 to 0.41.

Since gases flow bubbly and unsteadily through the bed in bubble flow, flow paths of water, i.e. channels, dynamically change. Figure 5 shows a mechanism of gas-flowing as bubble or slug. In a case of being packed with particles with a relatively large scale of the diameter, the intensity of capillary force decreases. That is, a volume of water held in pores among particles decreases. A gravity force easily affects water that is not held in pores as shown in Figure 5(b). Finally, the water divides air channels in the bed. When this phenomenon occurs here and there in the packed bed, gases flow like bubbles. It is considered that, at same value of S_w, an intensity of the *hydrodynamic dispersion* in bubble flow is higher than that in channel flow, since dynamic changes of water saturation locally occur in the bed. The bubble gases cause the dynamic and local changes of water saturation. However, the values of P_e take nearly the same values as those of channel flow in d_p=0.1. It follows from this that the dynamic change of water channels has no effect of emphasizing the *hydrodynamic dispersion*.

Breakthrough curves for d_p=0.06 disagree with the curves obtained by the *advection*-dispersion as shown in Figure 6. Haga et al. (1998) showed that this is due to a local distribution of water saturation in packed beds. The distribution of water saturation in packed beds may be microscopically heterogeneous even if water saturation is macroscopically homogeneous. It is considered that the *hydrodynamic dispersion* is strongly affected by the local distribution of saturation.

5. CONCLUSION

Tracer experiments in gas-liquid, two-phase flow through a porous media were carried out. The tracer tests were conducted under the following four flow conditions: single-phase flow, single-phase flow with entrapped gas, bubble flow, and channel flow. In each condition, the *hydrodynamic dispersion* coefficient (D_h) was obtained by being compared with the numerical model described by a one-dimensional advection-dispersion equation. In the relationship between the dispersion coefficient and water saturation, critical water saturation was observed and depended on whether or not the gas phase in the bed is mobile. Above the critical saturation, there was a single-phase (water) flow with entrapped gases and the dispersion coefficient linearly increased as S_w decreased. Below the critical saturation, water- and gas-phase flow (channel flow) appeared. The relationship was characterized by a steep increase in D_h as S_w decreases.

The bubble flow was observed when the particle diameter is relatively larger (d_p=0.2) in the experimental conditions of this study. Gases flow unsteadily in porous media as bubbles, so flow-paths of water dynamically change and become more complex. However, the dispersion coefficients show that the values for the bubble flow were nearly same as the value for the channel flow. It is found that the dynamic change of flow paths of water in bubble flow does not have serious effects on *hydrodynamic dispersion*.

Breakthrough curves for the relatively smaller diameter of glass beads (d_p=0.06) disagree with the curves obtained by the *advection*-dispersion. This is due to a local distribution of water saturation in packed beds. This study shows that the intensity of the effect of the local distribution of saturation is much higher than that of the effect of the dynamical change of the flow paths of water.

6. REFERENCES

Bear, J., *Dynamics of Fluids in Porous Media*, Elsevier, New York, 1972.

Bond W. J., and I. R. Philips, Cation exchange isotherms obtained with batch and miscible displacement techniques, *Soil Sci. Soc. Am. J.*, 54, 722-728, 1990.

Bond W. J., and P. J. Wierenga, Immobile water during solute transport in unsaturated sand columns, *Water Resour. Res*., 26(10), 2475-2481, 1990.

Chen, M. -R., R. E. Hinkley, and J. E. Killough, Computed tomography imaging of air sparging in porous media, *Water Resour. Res*., 32(10), 3013-3024, 1996.

de Smedt, F., and P. J. Wierenga, Approximate analytical solution for solute flow during infiltration and redistribution, *Soil Sci. Soc. Am. J.*, 42, 407-412, 1978.

de Smedt, F., and P. J. Wierenga, Mass transfer in porous media with immobile water, *J. Hydrol*. 41, 59-67, 1979a.

de Smedt, F., and P. J. Wierenga, A generalized solution for solute flow on soils with mobile and immobile water, *Water Resour. Res*., 15(5), 1137-1141, 1979b.

de Smedt, F., and P. J. Wierenga, Solute transfer through columns of glass beads, *Water Resour. Res*., 20(2), 225-232, 1984.

Gelhar, L. W., C. Welty, and K. R. Rehfeldt, A Critical Review of data on field-scale dispersion in aquifers, *Water Resour. Res*., 28(7), 1955-1974, 1992.

Haga, D., Y, Niibori, and T. Chida, A fundamental study on the response analysis of liquid tracer in gas-liquid, two-phase steady flow in porous media (in Japanese), *J. Geothermal Res., Soc*., Jpn., 20(4), 263-274, 1998.

Haga, D., Y, Niibori, and T. Chida, Hydrodynamic dispersion and mass transfer in Unsaturated flow., *Water Resour. Res.*, 35(4), 1065-1077, 1999.

Levenspiel, O., *Chemical Reaction Engineering*, Second Edition, John Wiley & Sons, Inc., New York, 1972.

Niibori, Y., A. Kounosu, and T. Chida, Fundamental study on tracer response analysis for water-steam flow accompanied by boiling in a porous medium, *J. Geothermal Res., Soc*., Jpn., 14(2), 129-144, 1992.

Niibori, Y., and T. Chida, A model of local distribution of saturation in a fractured layer, and its application, *Nineteenth Annual Workshop Geothermal Reservoir Engineering*, Stanford Univ., Stanford, California, Jan., 18-20, 1994.

Tetsu K. Tokunaga and Jiamin Wan, Water film flow along fracture surfaces of porous rock, *Water Resour. Res.*, 33(6), 1287-1295, 1997.

Wehner, J. F., and R. H. Wilhelm, Boundary conditions of flow reactor, *Chem. Eng. Sci*., 6, 89-93, 1956.

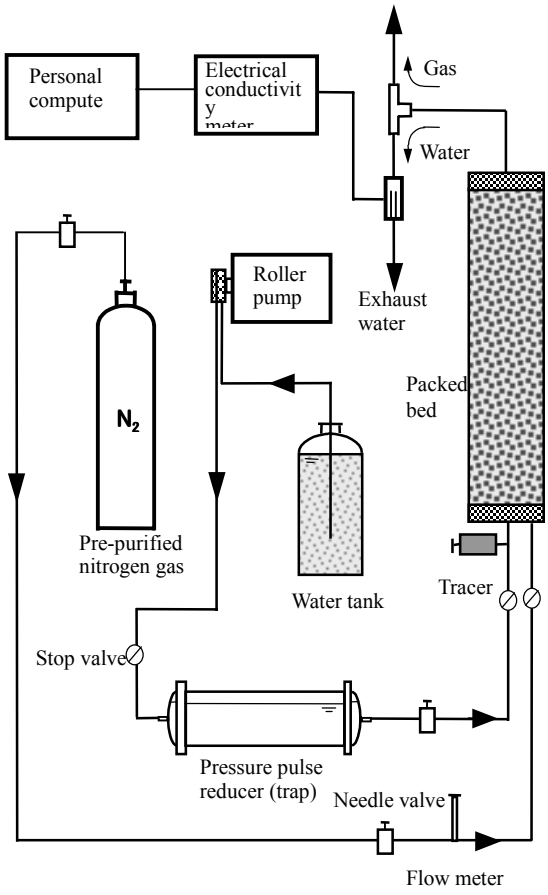

Figure 1. Schematic diagram of experimental apparatus.

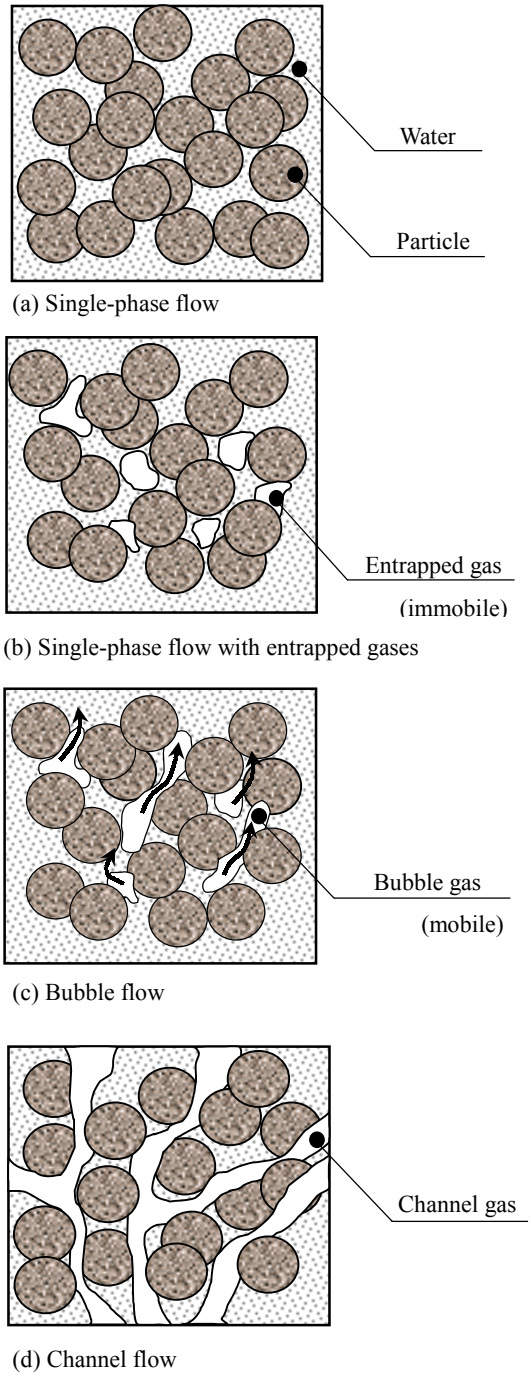

Figure 2. Schematic illustrations of fluids flow in porous media.

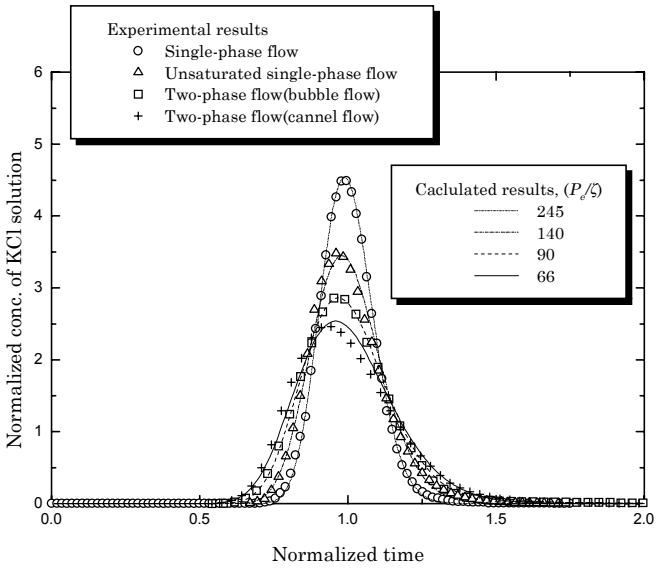

Figure 3. Experimental and numerical breakthrough curves

Table 1. Observed flow patterns of fluids and experimental conditions.

Particle diameter, d_p [cm]	Water saturation, S_w	Flow pattern (In figurer 2)
0.20	S_w =0.68	Fig. 2 (d)
	$\boldsymbol{S_w}$ =0.75,0.78,0.77	Fig. 2 (c)
	$\boldsymbol{S_w}$ =0.87	Fig. 2 (b)
	$\boldsymbol{S_w}$ =1	Fig. 2 (a)
0.10	S_w <0.75	Fig. 2 (d)
	0.73< S_w <1.00	Fig. 2 (b)
	S_w =1	Fig. 2 (a)
0.06	S_w <0.73	Fig. 2 (d)
	0.71< S_w <1.00	Fig. 2 (b)
	S_w =1	Fig. 2 (a)

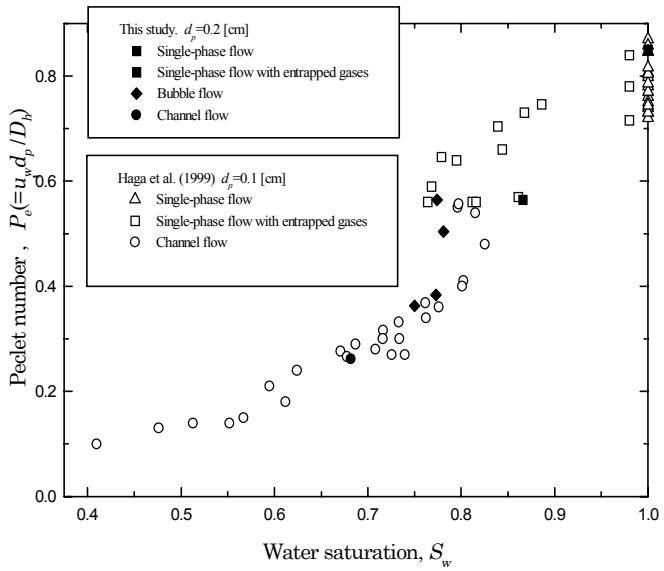

Figure 4. Relation ship between P_e and S_w.

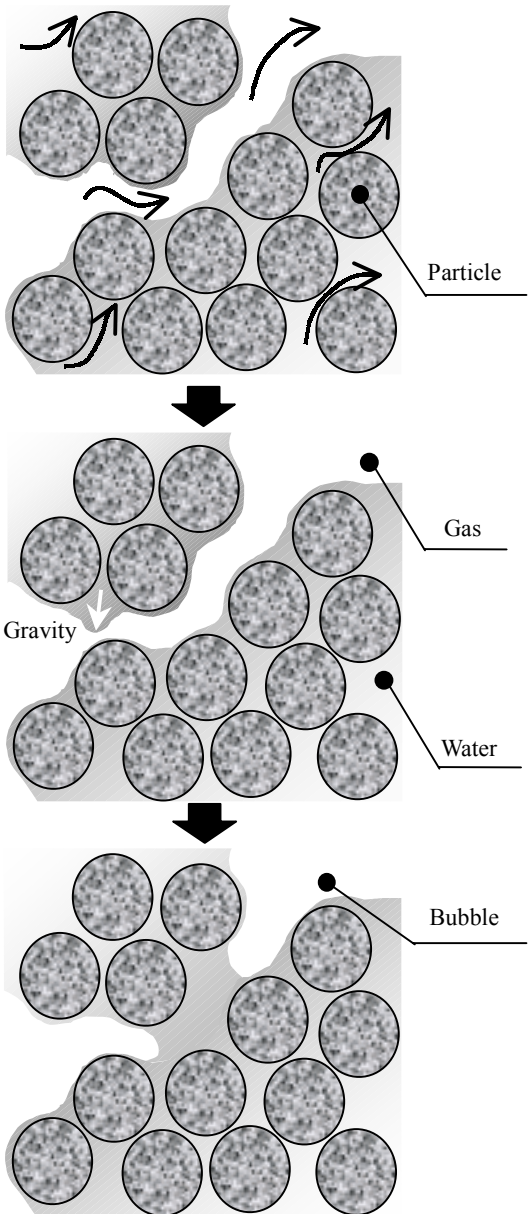

Figure 5. Schematic illustration of a mechanism of bubble flow.

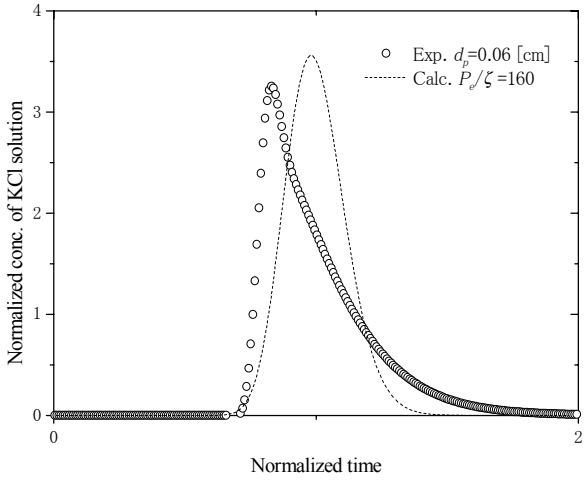

Figure 6. Experimental and numerical breakthrough curves at d_p=0.06.